

~~CONFIDENTIAL~~

Copy
RM H54I17

6

NACA RM H54I17



3 1176 00148 5862

NACA

RESEARCH MEMORANDUM

LIFT AND DRAG CHARACTERISTICS OF THE DOUGLAS X-3

RESEARCH AIRPLANE OBTAINED DURING

DEMONSTRATION FLIGHTS TO A

MACH NUMBER OF 1.20

By Donald R. Bellman and Edward D. Murphy

High-Speed Flight Station
Edwards, Calif.

CLASSIFIED DOCUMENT

This material contains information affecting the National Defense of the United States within the meaning of the espionage laws, Title 18, U.S.C., Secs. 793 and 794, the transmission or revelation of which in any manner to an unauthorized person is prohibited by law.

**NATIONAL ADVISORY COMMITTEE
FOR AERONAUTICS**

WASHINGTON

December 6, 1954

~~CONFIDENTIAL~~
UNCLASSIFIED

CLASSIFICATION CHANGED

UNCLASSIFIED

*Y. A. C. -
By authority of R.A. 12.9. Eff. 10/11/53. Date 7/17/53. 954*

[REDACTED]
NATIONAL ADVISORY COMMITTEE FOR AERONAUTICS

RESEARCH MEMORANDUM

LIFT AND DRAG CHARACTERISTICS OF THE DOUGLAS X-3
RESEARCH AIRPLANE OBTAINED DURING
DEMONSTRATION FLIGHTS TO A
MACH NUMBER OF 1.20

By Donald R. Bellman and Edward D. Murphy

SUMMARY

Lift and drag data were obtained during the manufacturer and Air Force demonstration flights of the Douglas X-3 airplane. The data covered the Mach number range from 0.82 to 1.20 with considerable variation in lift. The lift-curve slope increased from 0.085 deg⁻¹ at a Mach number of 0.82 to 0.115 deg⁻¹ near a Mach number of 1.0 and then decreased to about 0.093 deg⁻¹ in the supersonic region. For a lift coefficient of 0.20 the drag rise occurred at a Mach number of 0.92 and the value of drag coefficient at supersonic Mach numbers was about twice the value below the drag rise. The drag-due-to-lift factor had values between 0.20 and 0.23. The maximum lift-drag ratio varied from 7.2 at a Mach number of 0.82 to a constant value of 4.0 for Mach numbers from 1.05 to 1.20. A comparison of the flight data with wind-tunnel and rocket-model tests shows that the model tests satisfactorily predict the performance of the airplane.

INTRODUCTION

The X-3 airplane is one of the series of research airplanes constructed for flight tests being conducted under a joint Air Force, Navy, and National Advisory Committee for Aeronautics research program. It was designed for supersonic speeds and has a thin straight wing of low aspect ratio. The long pointed fuselage is large in comparison with the size of the wing. This paper presents lift and drag data from flights performed during the demonstration flights by Douglas Aircraft Co. and the Air Force. The data cover the Mach number range from 0.82 to 1.20 and at certain Mach numbers the lift coefficients range from

[REDACTED]

0 to 1. However, since the flights were made for structural demonstration purposes, the coverage of the speed and lift ranges is not uniform and the bulk of the data lies in the supersonic region. A comparison is made between the flight results and data from wind-tunnel and rocket-model tests. The flights were conducted at Edwards Air Force Base, Calif., in the period from June to December 1953.

SYMBOLS

A	tail-pipe exit area, sq ft
a_x	measured longitudinal acceleration, g units
C_D	drag coefficient, $\frac{D}{qS}$
C_f	thrust coefficient, $\frac{\text{Measured thrust}}{\text{Calculated thrust}}$
C_L	lift coefficient, $\frac{L}{qS}$
C_{L_α}	lift-curve slope, deg^{-1}
C_N	normal-force coefficient, $\frac{nW}{qS}$
C_X	longitudinal-force coefficient, $\frac{F_n - W a_x}{qS}$
D	drag along flight path, lb
dC_D/dC_L^2	drag-due-to-lift factor
F_j	jet thrust, lb
F_n	net thrust, lb
g	acceleration due to gravity, ft/sec^2
L	lift normal to flight path, lb

M	Mach number
M.A.C.	mean aerodynamic chord
N	engine speed, rpm
n	normal acceleration, g units
p	atmospheric pressure, lb/sq ft
P_6	static pressure at tail-pipe exit, lb/sq ft
P_{t_2}	total pressure at compressor face, lb/sq ft
P_{t_6}	total pressure at tail-pipe exit, lb/sq ft
q	dynamic pressure, lb/sq ft
S	wing area, sq ft
T	atmospheric temperature, °R
T_t	inlet air total temperature, °R
W	airplane weight, lb
w	engine air flow, lb/sec
α	angle of attack, deg
γ	ratio of specific heats
δ_c	altitude normalizing factor, $\frac{P_{t_2}}{2116}$
θ_c	temperature normalizing factor, $\frac{T_t}{518.4}$
L/D_{max}	maximum lift-drag ratio

AIRPLANE

The X-3 research airplane was built by the Douglas Aircraft Co. and is a single-place straight-wing airplane, powered by two J34 turbojet engines equipped with afterburners. It has a long pointed fuselage that has a large frontal area in comparison with the size of the wing. The wing has an aspect ratio of 3.09, is unswept at the 75 percent chord line, and is equipped with both leading- and trailing-edge flaps. Its thickness is 4.5 percent of the chord length and the section is hexagonal with sharp leading and trailing edges, but with the four obtuse vertices rounded.

Photographs of the airplane are presented in figure 1 and a three-view sketch showing primary dimensions is presented in figure 2. Additional dimensions and specifications are given in table I.

INSTRUMENTATION

The X-3 airplane is equipped with standard NACA recording instruments for measuring airspeed, pressure altitude, angle of attack, accelerations, outside air temperature, the various pressures needed for the thrust calculations, stabilizer position, and other items not pertinent to this paper. The engine speeds and tail-pipe eyelid positions were recorded by means of a photopanel and 35-mm camera. A timing system accurately synchronized all films.

Figure 3 is a sketch of the nose boom showing the location of the total and static pressure orifices and the angle-of-attack and angle-of-yaw vanes. The slanted pressure probes on the nose of the boom were part of the Douglas Aircraft Co. instrumentation and were not used for the data of this paper. The outside air temperature was measured by a shielded resistance-type thermometer that projected downward from the nose-wheel door.

Tail-pipe total head was measured at the afterburner inlet and consisted of 3 radial rakes having 5 probes each. All 15 probes on each engine were then manifolded and connected to a single manometer cell. At the compressor inlet there are 4 rakes with 4 probes each for measuring total pressure and each probe was connected to a separate manometer cell. To avoid the large amount of work that would be involved in arithmetically averaging the values, the probe on each engine that most nearly represented the average for that engine during a representative flight was selected and used for all subsequent flights.

THRUST AND DRAG CALCULATIONS

The net thrust of the engines was considered to be the force resulting from the change in momentum of the air and fuel actually passing through the engines. The effect of boundary bleed air and engine cooling air, which properly should be credited to the engines, was credited to the airplane because of insufficient instrumentation. It is hoped that this effect can be measured during subsequent tests. The jet thrust which is the momentum force at the tail-pipe exit was calculated by using the formula

$$F_j = C_f A \left\{ p_6 \left(\frac{2\gamma}{\gamma - 1} \right) \left[\left(\frac{p_{t6}}{p_6} \right)^{\frac{\gamma-1}{\gamma}} - 1 \right] + p_6 - p \right\}$$

For subsonic tail-pipe velocities, which occurred during the low-speed maneuvers, the tail-pipe static pressure p_6 was assumed equal to the atmospheric pressure p , which reduced the formula to

$$F_j = C_f A p \left(\frac{2\gamma}{\gamma - 1} \right) \left[\left(\frac{p_{t6}}{p} \right)^{\frac{\gamma-1}{\gamma}} - 1 \right]$$

For sonic tail-pipe velocities the tail-pipe total pressure p_{t6} divided by the tail-pipe static pressure p_6 was assumed equal to the critical pressure ratio as defined by theoretical relationships:

$$\frac{p_{t6}}{p_6} = \left(\frac{\gamma + 1}{2} \right)^{\frac{\gamma}{\gamma-1}}$$

The formula for thrust then becomes

$$F_j = C_f A \left[p_{t6} \left(\frac{2}{\gamma + 1} \right)^{\frac{\gamma}{\gamma - 1}} (\gamma + 1) - p \right]$$

The equation can be further reduced by inserting a value for γ which is assumed to be 1.33 for afterburner-off conditions and 1.25 for afterburner-on conditions. However, the equation is very insensitive to variations in γ and a mean value can be used and cause an error that is considerably less than 1 percent. Thus the formula becomes

$$F_j = C_f A (1.254 p_{t6} - p)$$

The thrust coefficient C_f normally is taken to be the ratio of true thrust as measured by a thrust stand to the jet thrust as determined by the tail-pipe pressure measurements. No adequate thrust stand runs were made during the period of these tests, so a value of 1.00 was assumed.

The ram drag, which is the inlet momentum force, must be subtracted from the jet thrust to obtain the net engine thrust. It is obtained by multiplying the true airplane velocity and the mass flow of air through the engines. The engine air flow is determined by considering the engine to be a constant volume pump at any given normalized engine speed. A plot of normalized air flow $w\sqrt{\theta_c}/\delta_c$ against normalized engine speed $N/\sqrt{\theta_c}$ was obtained from the manufacturer for a standard J34-WE-17 engine and used for all tests. The pressure normalizing factor was based on the total pressure measured at the compressor inlet and the temperature normalizing factor was based on the outside air total temperature. The outside air static temperature necessary for the determination of true airplane velocity was obtained using the following relationship

$$T = \frac{T_t}{1 + 0.198M^2}$$

The accelerometer method was used to determine the drag forces and the following equations were used to calculate the lift and drag coefficients:

$$C_L = C_N \cos \alpha - C_X \sin \alpha$$

$$C_D = C_X \cos \alpha + C_N \sin \alpha$$

ACCURACY

The data of this paper are not as accurate as would be obtained if special flights were made for the purpose of producing lift and drag data. It was not practical to make elaborate flight calibrations of the angle-of-attack measuring system nor to install an extra-sensitive longitudinal accelerometer. However, since many of the errors are random the amount of error is reduced by fairing a curve through a large number of points, particularly when the data come from several flights and runs as was the case for most of the curves. Although greater accuracy would be desirable, the accuracy obtained under the conditions of these tests is considered sufficiently satisfactory to show the trends and the general order of magnitude of the values and to indicate approximately the merit of the various preliminary model tests.

The airspeed installation was calibrated using the radar-phototheodolite method described in reference 1, and on the basis of this calibration the Mach numbers given in this paper are accurate within ± 0.01 . The angle-of-attack system was calibrated only under static ground conditions, hence would be subject to errors from vane floating, boom and fuselage bending, and upwash. Generally, data points where pitching velocity was appreciable were not used, and when necessary to use such data corrections were made for the effective change in airstream direction.

The measurement of the thrust involved several inaccuracies. Tail-pipe total head was measured ahead of the afterburner flame holder and fuel injector rings, and this procedure neglects the total head losses of these obstructions. The effects of the cooling air ejectors were also neglected. A small portion of the data was taken from runs where only the right-hand engine was instrumented for thrust. Data from such runs were taken only where the speed of both engines and other conditions were comparable.

The measurement of longitudinal acceleration which has an important bearing on the drag coefficients was made with a standard three-component NACA accelerometer which has an accuracy of $\pm 0.025g$.

Because all the aforementioned sources of error affect the values of drag coefficient, it is very difficult to estimate the absolute accuracy. However, the Mach number for the drag rise and the relative magnitude of the drag rise should be substantially correct.

TESTS, RESULTS, AND DISCUSSION

The data presented in this paper were obtained during the demonstration flights by the Douglas Aircraft Co. and the Air Force. The maneuvers performed consisted of level runs, high-speed dives, and pull-ups. Most of the data were taken in the altitude range from 25,000 to 35,000 feet, although one run extended as low as 14,500 feet and another as high as 37,500 feet. The Reynolds number for the tests, based on the mean aerodynamic chord, varied from 13×10^6 to 37×10^6 .

Data are presented for 12 approximately constant Mach numbers ranging from 0.82 to 1.20. The data covered a narrow range of Mach number about each given Mach number and this range was ± 0.02 for a Mach number of 0.82, and ± 0.01 for Mach numbers of 0.90 and greater. Three of the twelve sets of constant Mach number data consisted of data from a single maneuver, whereas the other nine sets utilized data from two to ten maneuvers.

The variation of lift with angle of attack for the 12 Mach numbers is shown in figure 4. For these data the horizontal tail incidence varied with lift with the extreme values ranging from -1° to -8° . Below a lift coefficient of about 0.7 there was approximately a straight-line variation of lift with tail incidence.

The lift-curve slopes within the lift-coefficient range from 0.2 to 0.4 were determined from the data of figure 4 and are presented in figure 5. At a Mach number of 0.82 the lift curve had a slope of about 0.085 deg^{-1} which increased to a value of 0.115 deg^{-1} near a Mach number of 1.0 and then decreased to a value of about 0.093 deg^{-1} in the supersonic region.

The variation of drag coefficient with lift coefficient for the 12 Mach numbers is shown in figure 6 and a cross plot of these data is presented in figure 7 as the variation of drag coefficient with Mach number for constant values of lift coefficient. For a lift coefficient of 0.3 the drag coefficient was about 0.044 below the drag rise and increased to a value of 0.094 in the supersonic region. The drag-rise Mach number, when defined as the Mach number where the

slope of the curve becomes 0.10, had a value of about 0.92 for a lift coefficient of 0.20 and this decreased to about 0.90 at a lift coefficient of 0.40.

The data of figure 6 were plotted as drag coefficient against the square of the lift coefficient. The curves were approximately rectilinear for lift coefficients up to 0.6. The slopes, drag-due-to-lift factors, were measured and are presented in figure 8. There was only a slight variation with Mach number and all the values lay between 0.20 and 0.23.

The maximum lift-drag ratios determined for the various Mach numbers are presented in figure 9 along with the lift coefficient at which they occur. At a Mach number of 0.82 the maximum lift-drag ratio had a value of 7.2 which decreased with increasing Mach number and reached a constant value of about 4.0 for Mach numbers between 1.05 and 1.20. The lift coefficient at which the maximum lift-drag ratio occurred varied from about 0.35 at a Mach number of 0.82 to about 0.60 at a Mach number of 1.20.

The flight data have been compared with data from wind-tunnel tests (ref. 2) and rocket-model tests (ref. 3) and the results are presented in figure 10. The lift-curve slopes are compared at a lift coefficient of 0.3 and the drag data are compared at the same lift coefficient. The horizontal tail incidence was 0° for the wind-tunnel data, either -2.8° or -1.2° for the rocket-model data, and varied within the range of $-3.0^\circ \pm 1.5^\circ$ as required for trim in the flight tests. The lift-curve slopes of the three sets of data show the same general trends. The agreement of the drag data is satisfactory since the only point where there is appreciable difference is during the drag rise where the measurements are less certain. The maximum lift-drag ratio for the flight data is slightly higher than the model data in the subsonic region but agrees quite well with the wind-tunnel data in the supersonic region.

The comparison of the flight and model data shows that the model tests adequately predict the performance of the actual airplane. The comparison also indicates the merit of the flight tests since these demonstration flight tests gave a more adequate coverage of the Mach number and lift ranges than did either the rocket-model or wind-tunnel tests.

SUMMARY OF RESULTS

The lift and drag measurements made on the X-3 airplane during demonstration flights which covered the Mach number range from 0.82 to 1.20 showed the following results:

1. The lift-curve slope in the vicinity of a lift coefficient of 0.3 increased from 0.085 deg^{-1} at a Mach number of 0.82 to 0.115 deg^{-1} near a Mach number of 1.0 and then decreased to about 0.093 deg^{-1} in the supersonic region.

2. For a lift coefficient of 0.20 the drag rise occurred at a Mach number of 0.92 and the value of drag coefficient at supersonic Mach numbers was about twice the value below the drag rise.

3. The drag-due-to-lift factors varied only slightly with Mach number and had values between 0.20 and 0.23.

4. The maximum lift-drag ratio varied from 7.2 at a Mach number of 0.82 to a constant value of 4.0 for Mach numbers from 1.05 to 1.20.

5. A comparison of the flight data with data from wind-tunnel and rocket-model tests shows that the model tests adequately predict the performance of the airplane.

High-Speed Flight Station,
National Advisory Committee for Aeronautics,
Edwards, Calif., September 7, 1954.

REFERENCES

1. Zelovcik, John A.: A Radar Method of Calibrating Airspeed Installations on Airplanes in Maneuvers at High Altitudes and at Transonic and Supersonic Speeds. NACA Rep. 985, 1950. (Supersedes NACA TN 1979.)
2. Olson, Robert N., and Chubb, Robert S.: Wind-Tunnel Tests of a 1/12-Scale Model of the X-3 Airplane at Subsonic and Supersonic Speeds. NACA RM A51F12, 1951.
3. Peck, Robert F., and Hollinger, James A.: A Rocket-Model Investigation of the Longitudinal Stability, Lift, and Drag Characteristics of the Douglas X-3 Configuration With Horizontal Tail of Aspect Ratio 4.33. NACA RM L53F19a, 1953.

TABLE I.- PHYSICAL CHARACTERISTICS OF THE DOUGLAS X-3 AIRPLANE

Wing:	
Area, sq ft	166.5
Span, ft	22.69
Aspect ratio	3.09
Airfoil section	Modified hexagon
Airfoil thickness ratio, percent chord	4.5
Airfoil leading- and trailing-edge angles, deg	8.58
Mean aerodynamic chord, ft	7.84
Root chord, ft	10.58
Tip chord, ft	4.11
Taper ratio	0.39
Sweep at 0.75 chord line, deg	0
Incidence, deg	0
Dihedral, deg	0
Horizontal tail:	
Area, sq ft	43.24
Span, ft	13.77
Aspect ratio	4.38
Airfoil section	Modified hexagon
Airfoil thickness ratio at root chord, percent chord	8.01
Airfoil thickness ratio outboard of station 26, percent chord	4.5
Mean aerodynamic chord, ft	3.34
Taper ratio	0.405
Sweep at leading edge, deg	21.14
Sweep at trailing edge, deg	0
Dihedral, deg	0
Vertical tail:	
Area, sq ft	23.73
Span, ft	5.59
Aspect ratio	1.315
Airfoil section	Modified hexagon
Airfoil thickness ratio, percent chord	4.5
Mean aerodynamic chord, ft	4.69
Taper ratio	0.292
Sweep at leading edge, deg	45.0
Fuselage:	
Length, including boom, ft	66.75
Maximum width, ft	6.08
Maximum height, ft	4.81
Base area, sq ft	7.94
Power plant:	
Engines	Two J34-WE-17 with afterburner
Rating, each engine:	
Static sea-level military thrust, lb	3370
Static sea-level maximum thrust, lb	4850
Weight:	
Basic (without fuel, oil, water, pilot), lb	16,120
Total, lb	22,100

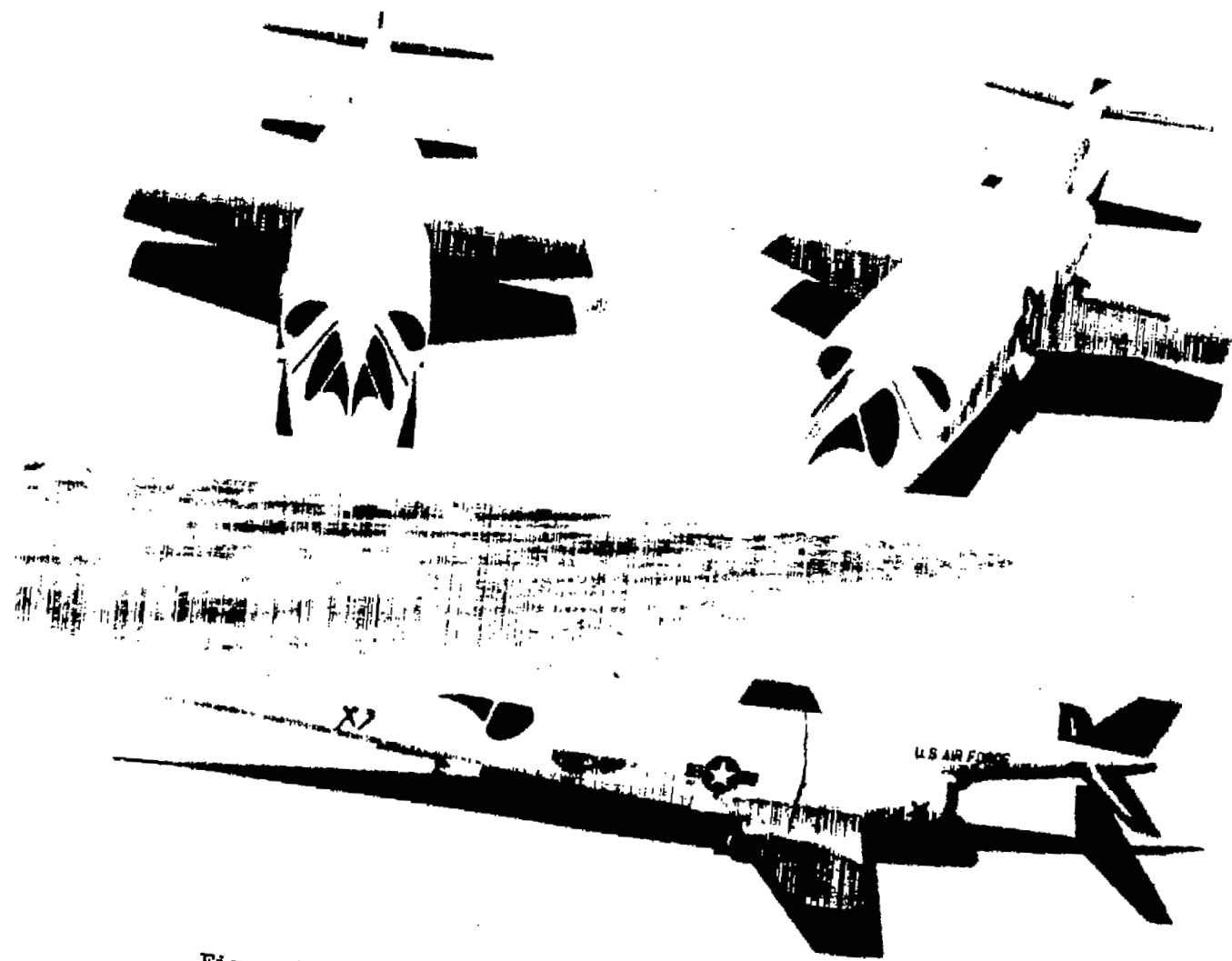


Figure 1.- Photographs of Douglas X-3 research airplane.

LE1228

NACA RM H54117

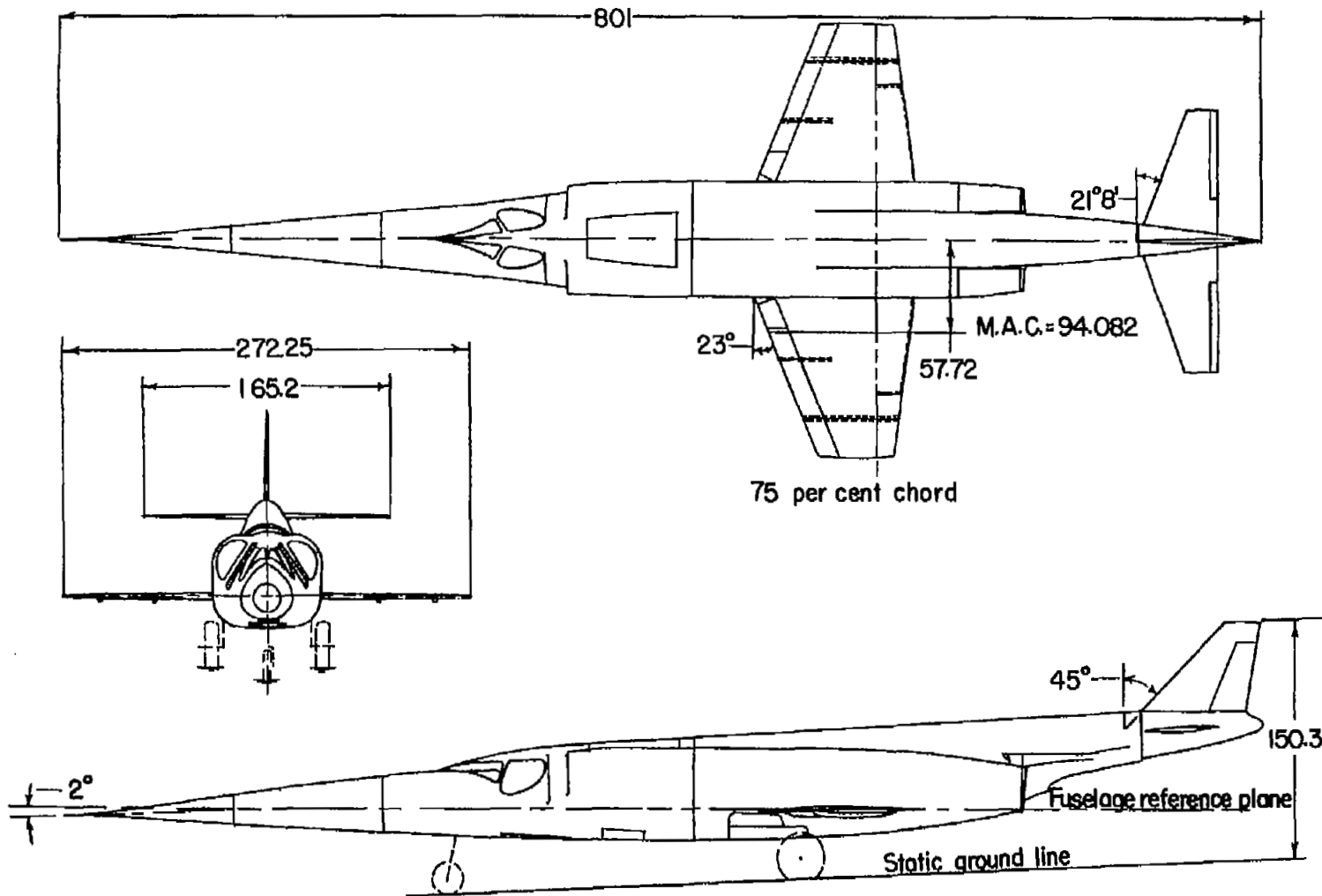


Figure 2.- Three-view drawing of X-3 airplane. All linear dimensions are in inches.

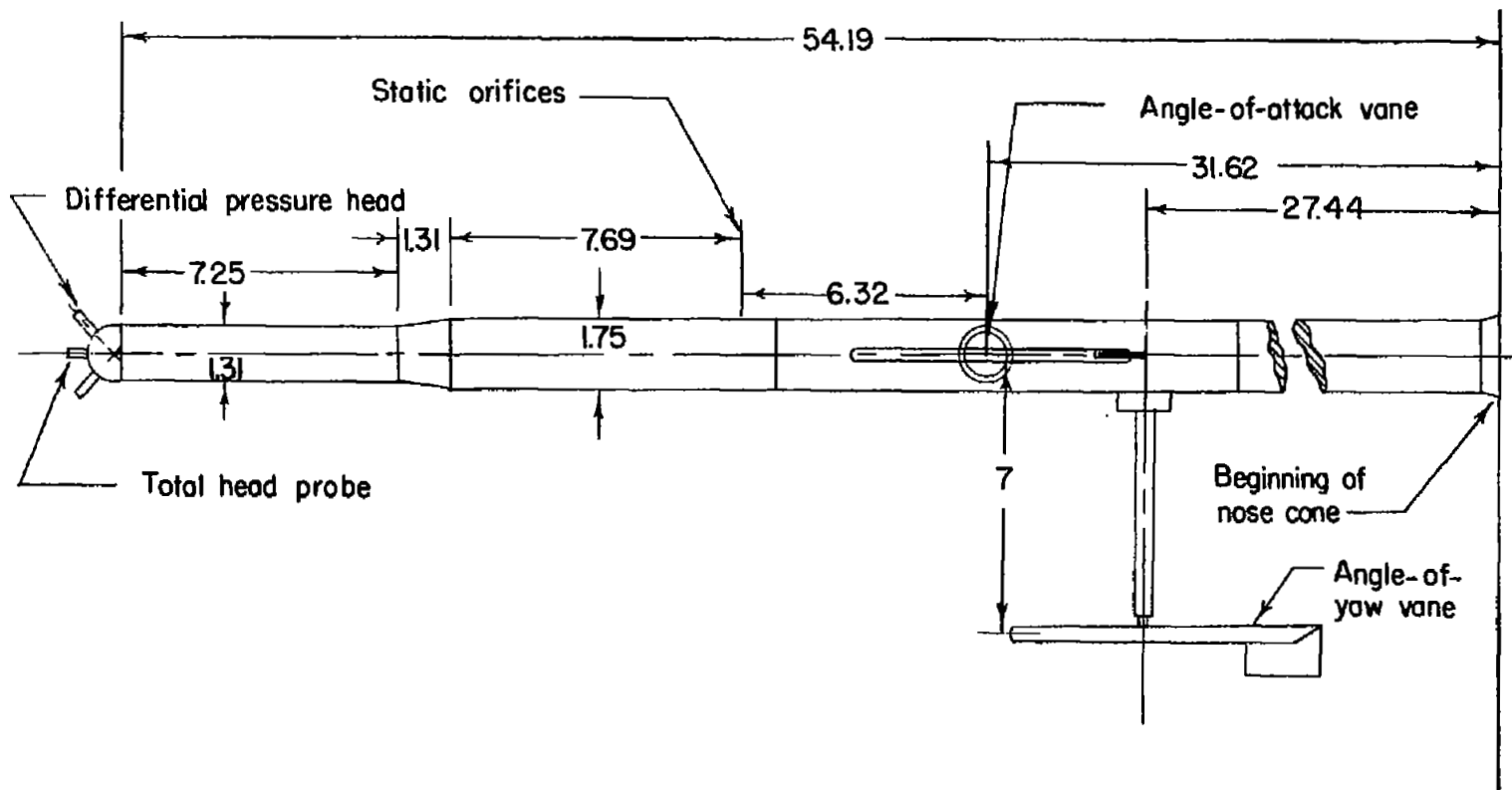


Figure 3.- Combined airspeed - angle-of-attack boom. All dimensions are in inches.

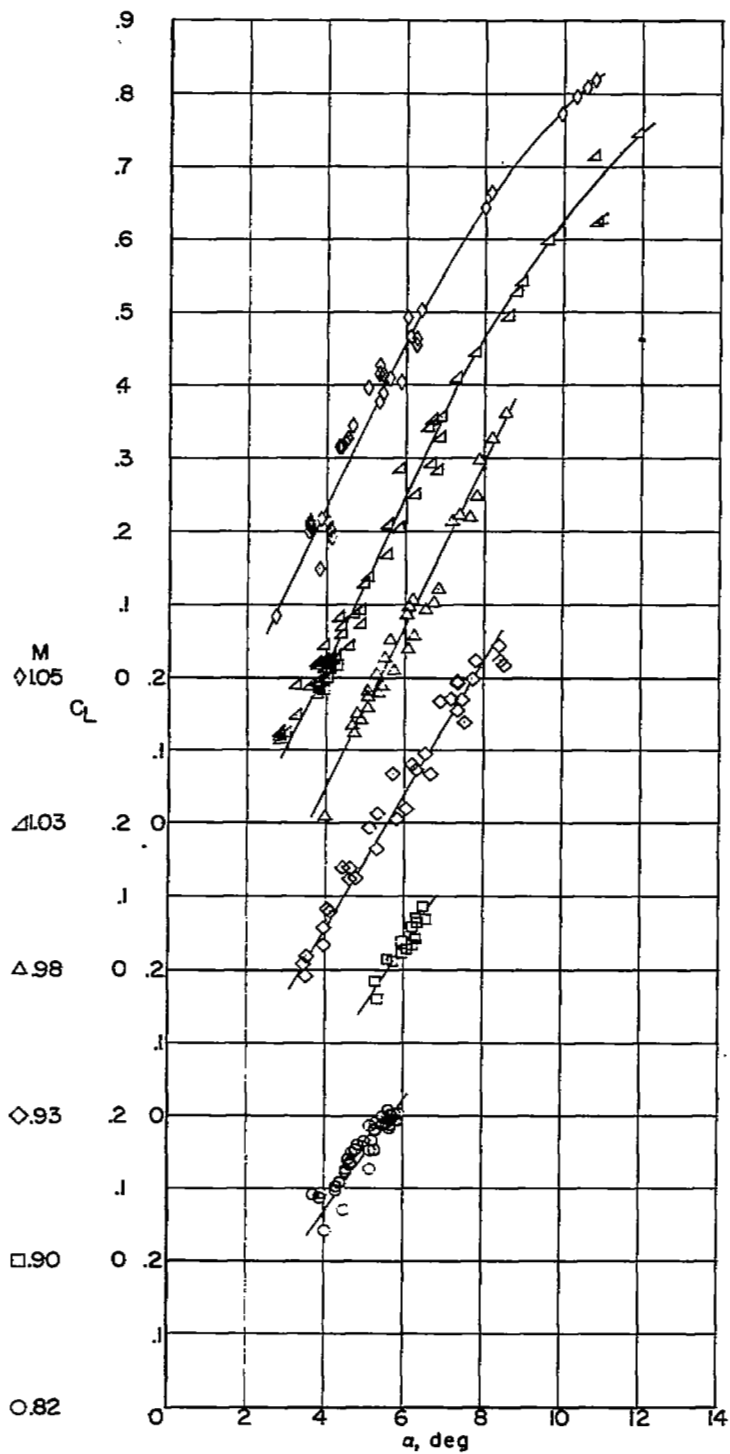


Figure 4.- Variation of lift coefficient with angle of attack for various constant Mach numbers.

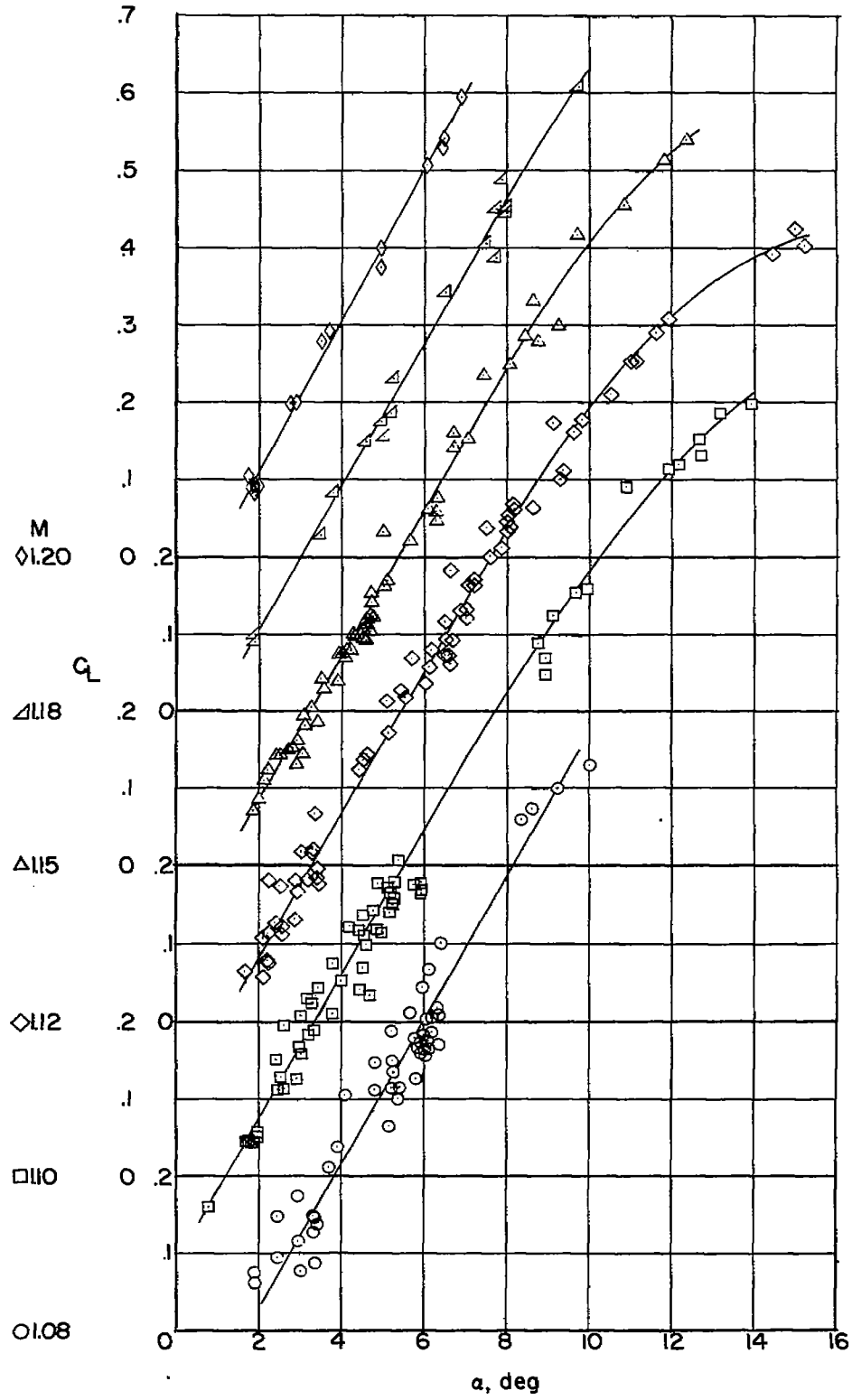


Figure 4.- Concluded.

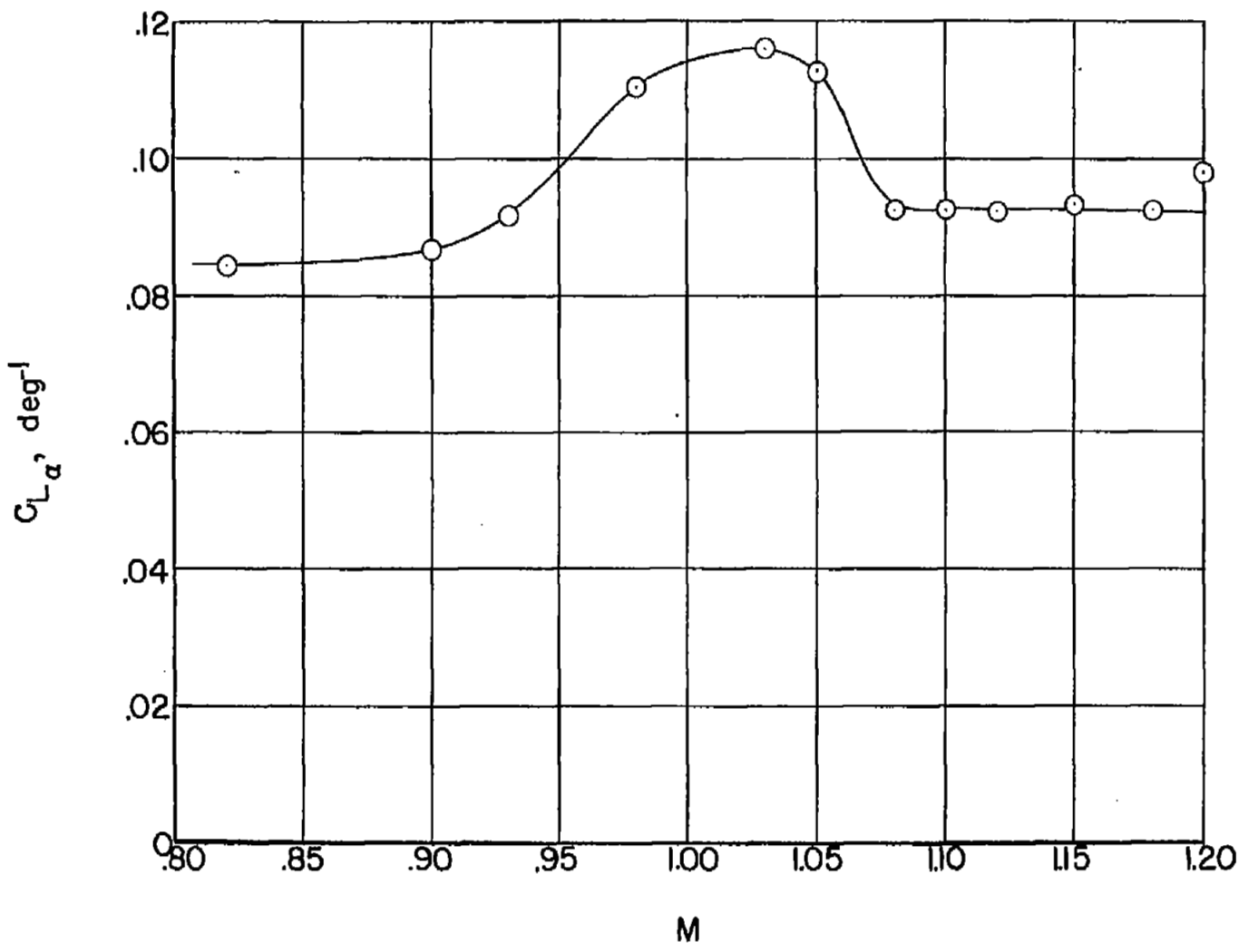


Figure 5.- Variation of lift-curve slopes with Mach number. $C_L \approx 0.3$.

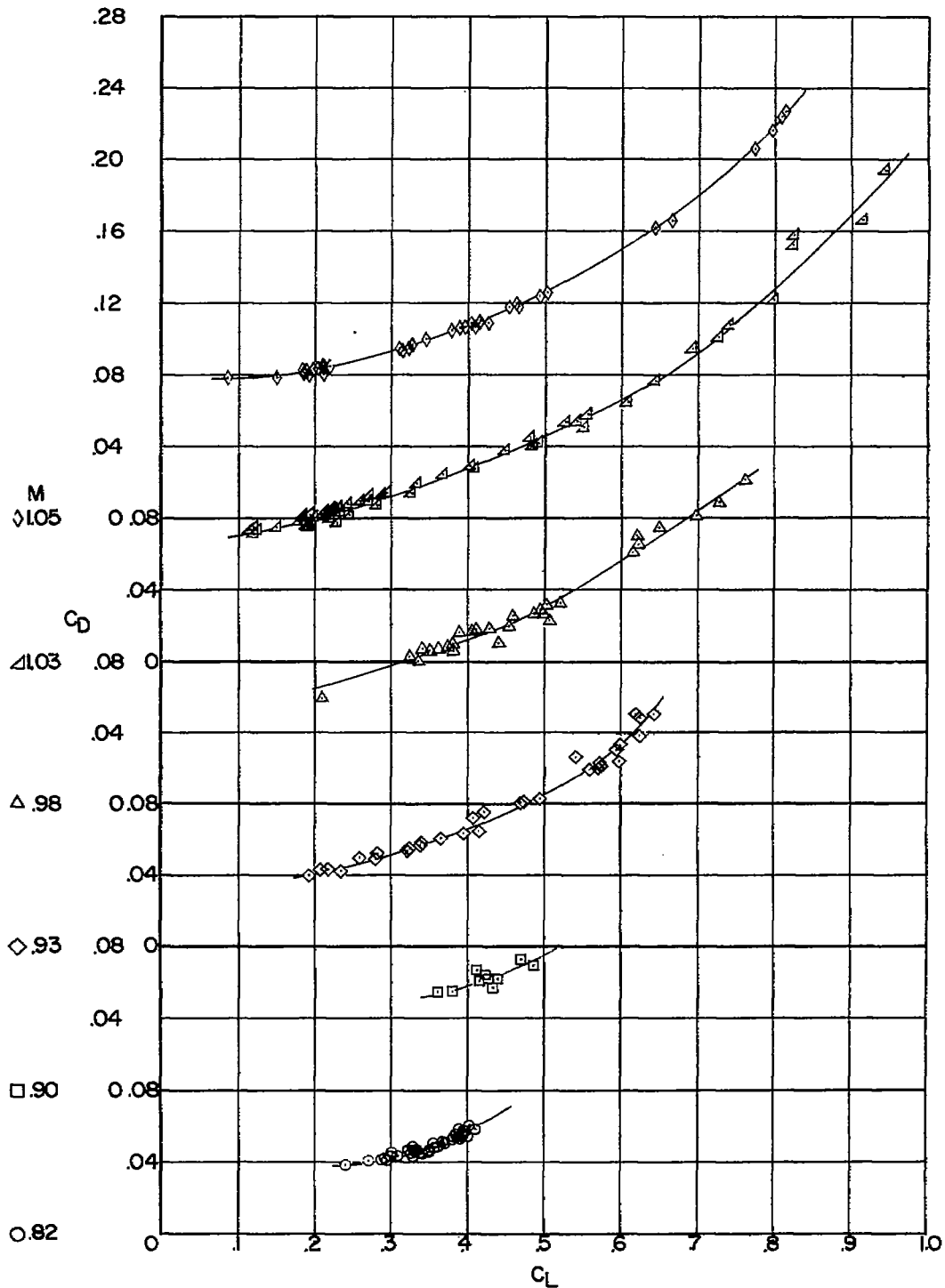


Figure 6.- Variation of drag coefficient with lift coefficient for various constant Mach numbers.

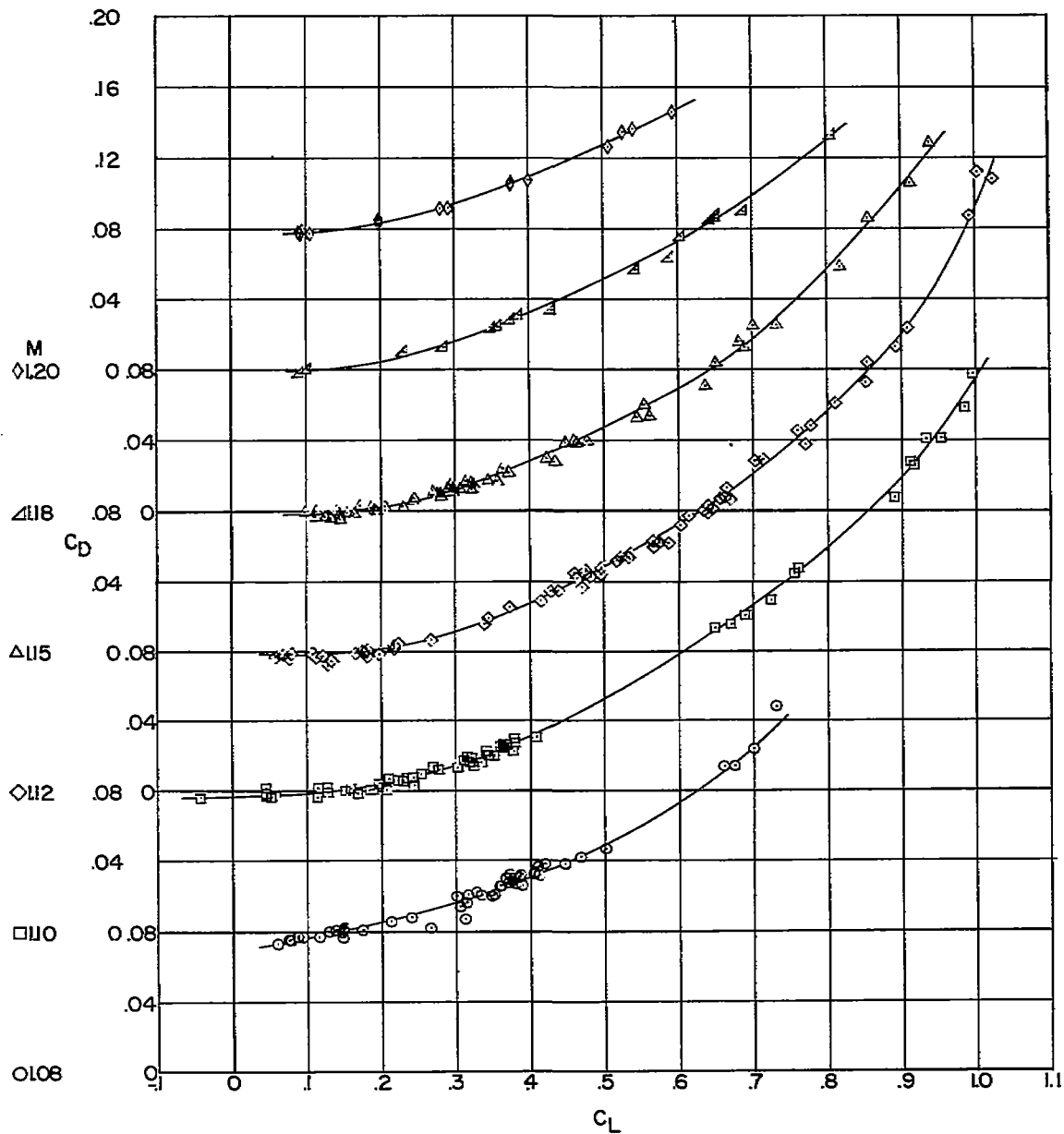


Figure 6.- Concluded.

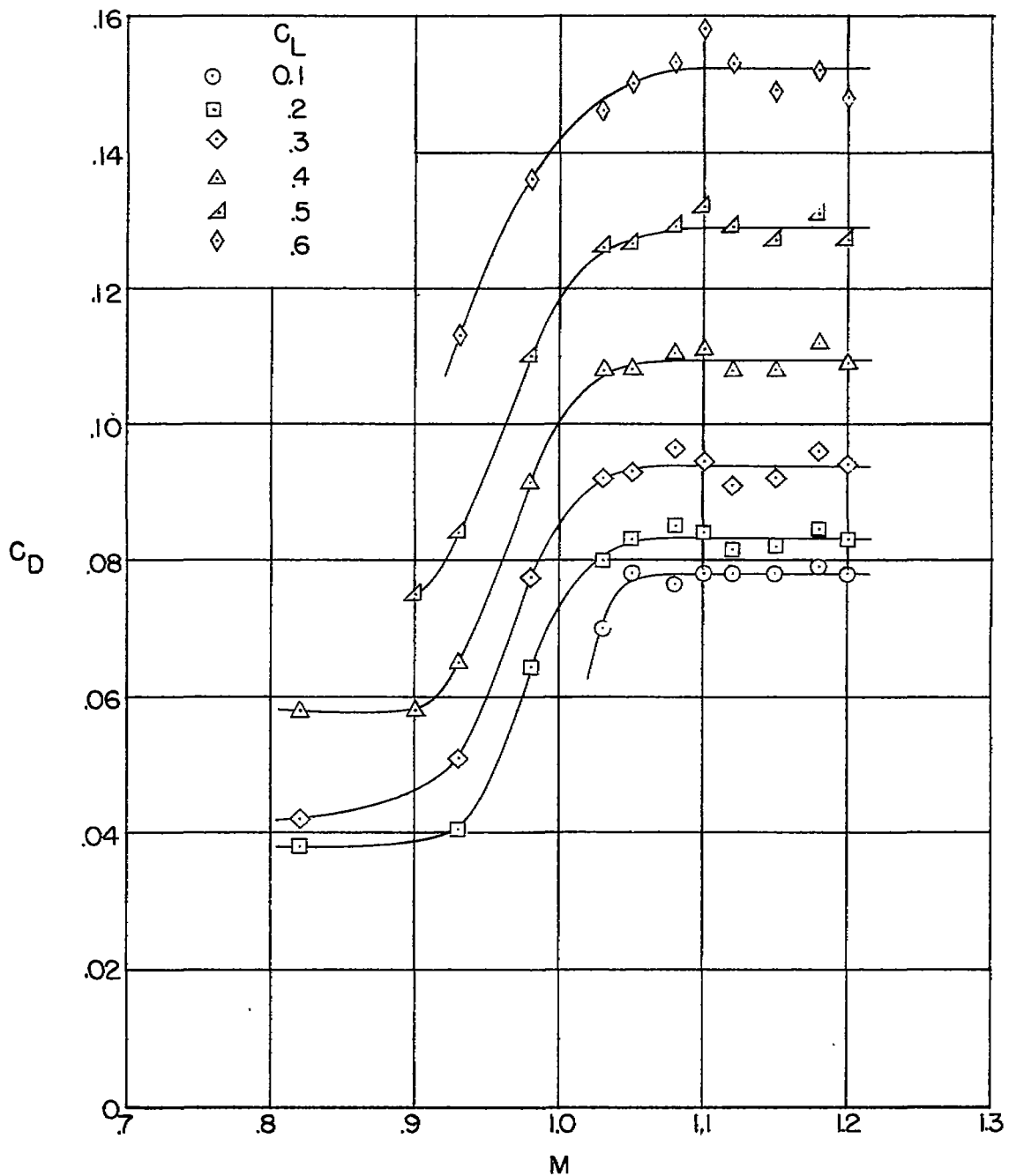


Figure 7.- Variation of drag coefficient with Mach number for constant values of lift coefficient.

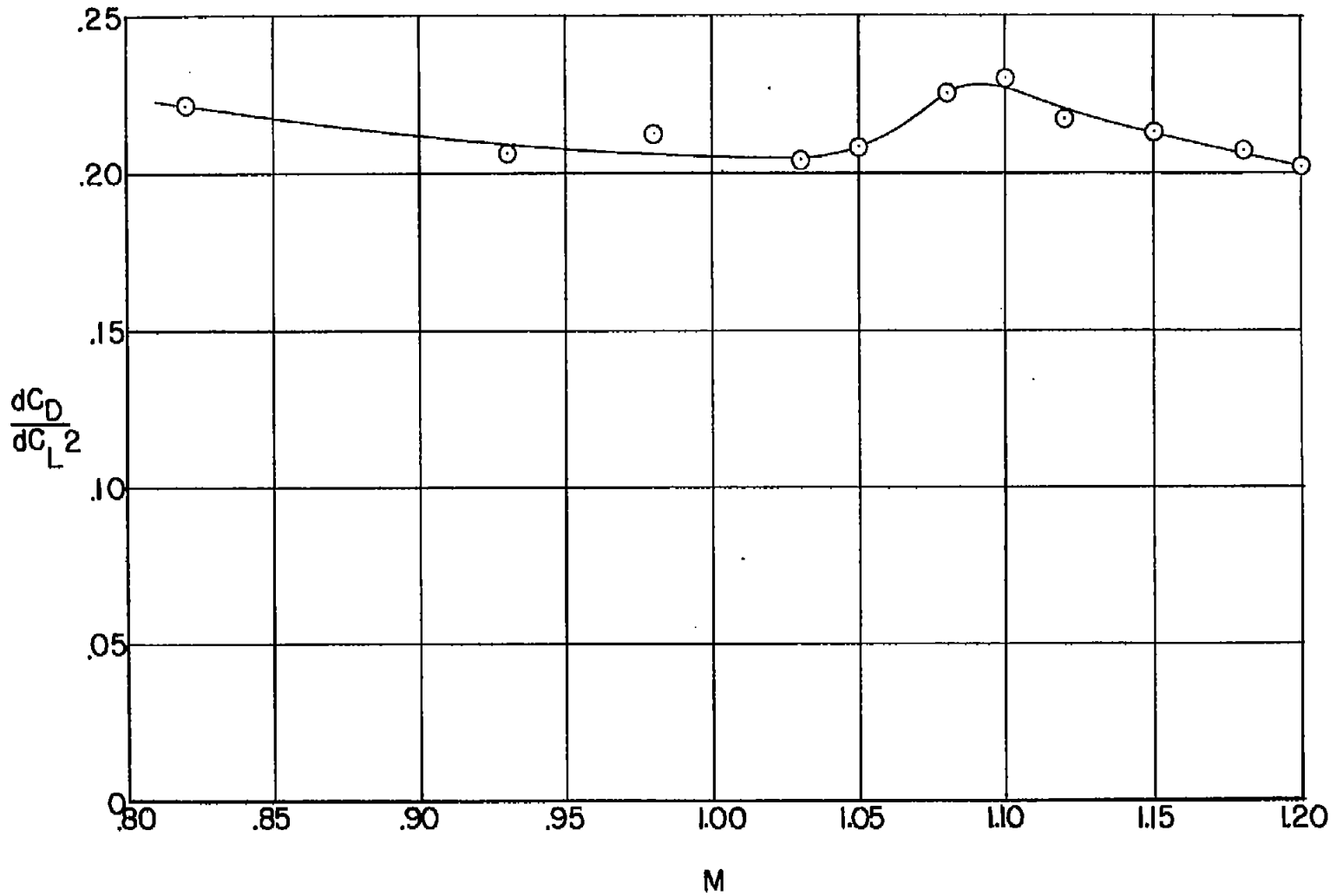


Figure 8.- Variation of drag-due-to-lift factor with Mach number.

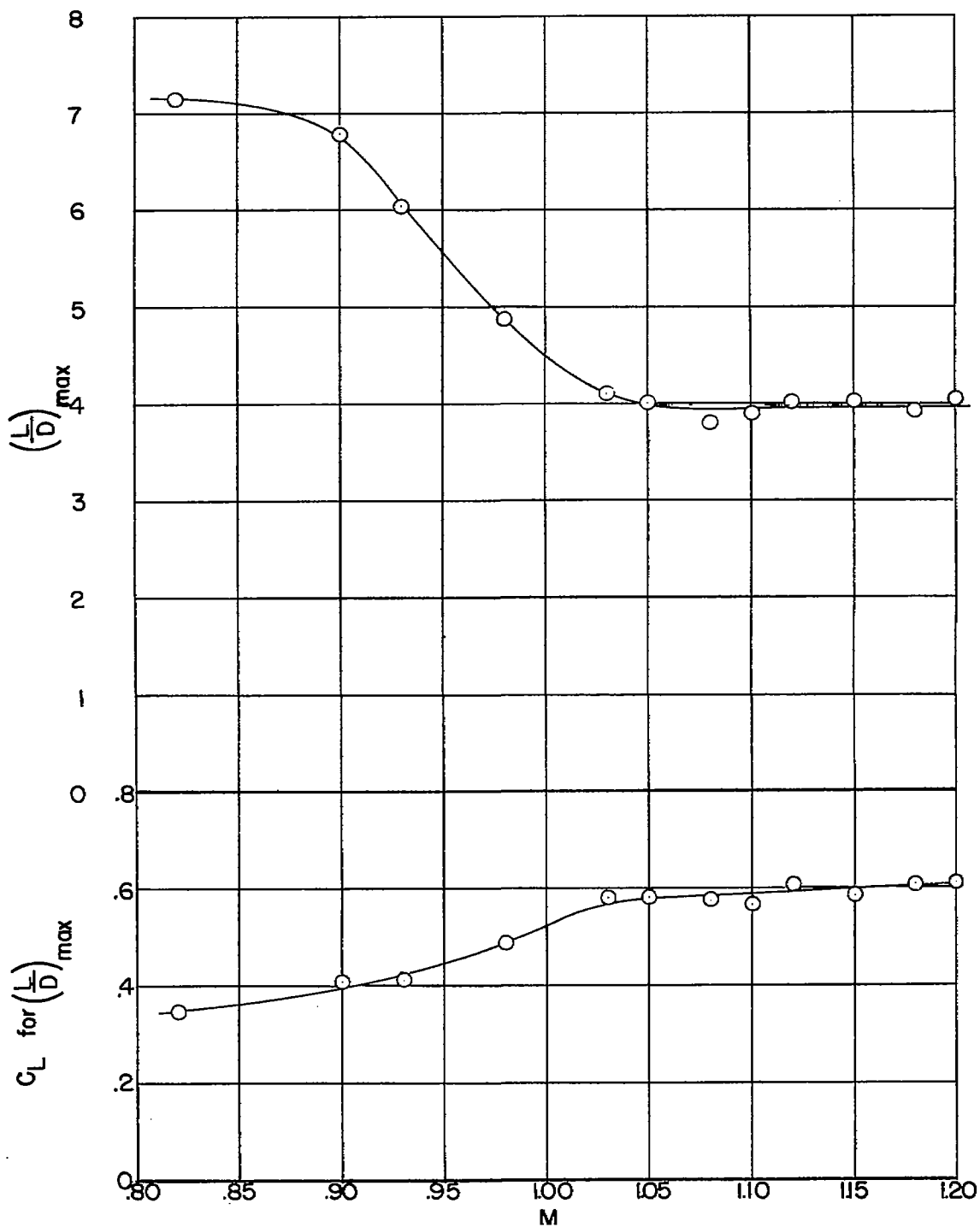


Figure 9.- Variation of maximum lift-drag ratio and corresponding lift coefficient with Mach number.

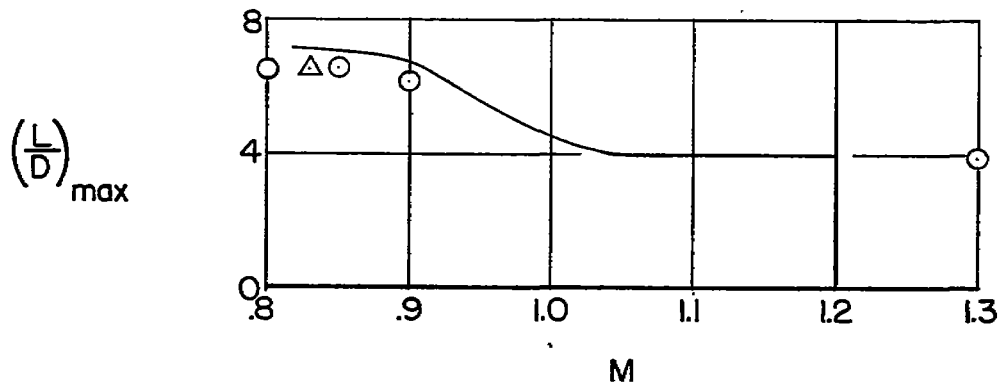
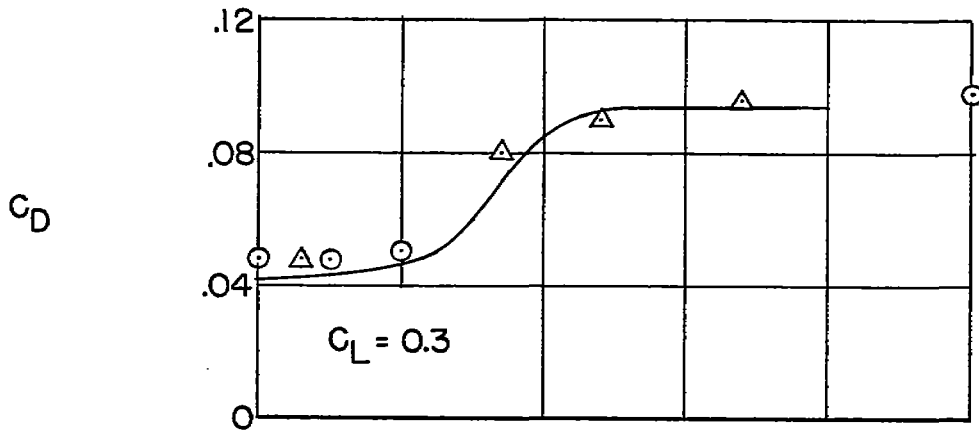
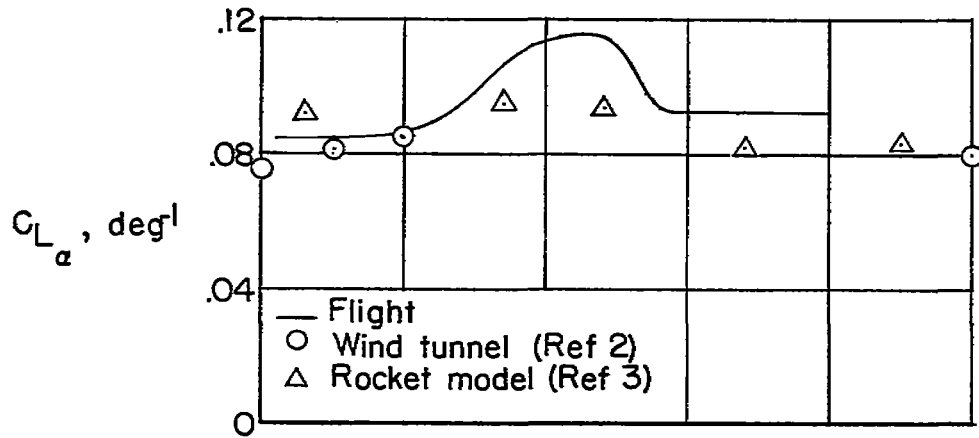


Figure 10.- Comparison of flight with wind-tunnel and rocket-model data.